

# Time-resolved Rayleigh scattering of excitons: Evidence for level repulsion in a disordered system

Vincenzo Savona

*Physics Department—IMO, Swiss Federal Institute of Technology Lausanne, CH-1015 Lausanne—EPFL, Switzerland*

Roland Zimmermann

*Institut für Physik der Humboldt Universität zu Berlin, Hausvogteiplatz 5-7, D-10117 Berlin, Germany*

(Received 18 December 1998)

The theory of resonant Rayleigh scattering of light by excitons in a disordered quantum structure is presented. Disorder is modeled by a random Gauss distributed potential with finite correlation length in space. The time dependent scattered signal under pulsed excitation is studied by solving the Schrödinger equation for the exciton center-of-mass motion. The key quantity turns out to be the distribution of energy level distances weighted by the optical matrix elements. The limit of classical center-of-mass motion is derived analytically, while large-scale simulations are performed for the general case. The results show that the quantum-mechanical nature of the exciton motion is responsible for an oscillating behavior of the time dependent intensity. The oscillations originate from an interplay between the quantum-mechanical energy-level repulsion and the correlation induced by the finite correlation length of the disorder. [S0163-1829(99)10031-6]

## I. INTRODUCTION

The elastic scattering of light (Rayleigh scattering) by a spatially inhomogeneous system is resonantly enhanced when spectrally close to an optical transition.<sup>1</sup> In the case of semiconductor quantum wells (QW's), the resonant Rayleigh scattering (RRS) by excitons has drawn particular attention in recent years. In fact, the RRS into nonspecular directions is directly connected to the presence of disorder in the QW plane and to the localization of the excitonic wave functions. Thus RRS can in principle provide important information about the nature of the exciton wave functions in presence of disorder. The early experimental results on QW's were obtained under steady-state excitation, allowing to resolve the spectral features of RRS. In particular, the pioneering work by Hegarty and co-workers<sup>2,3</sup> were focused at the detection of a "mobility edge" for the exciton center-of-mass (COM) motion. This feature was inferred from the frequency dependence of the exciton homogeneous linewidth that was derived from the RRS spectrum by means of a simple model for the light-scattering process. The same scheme has been subsequently adopted by other authors.<sup>4,5</sup> Although the existence of a mobility edge at frequencies within the exciton resonance has always represented a major controversy, these early investigations agreed on the fact that the RRS mainly originates from exciton states localized in the QW plane. More recently, the steady-state RRS measurement by Garro *et al.*<sup>6</sup> have provided information on the role of the typical correlation length characterizing the in-plane disorder. By comparing RRS and absorption spectra from samples obtained using different fabrication processes, they have argued that the technique of growth interruption at the interfaces produces disorder with a correlation length larger than the exciton Bohr radius. The fact that RRS originates mainly from exciton states localized on the subwavelength scale is actually well established. None of these studies, however, has provided information about the nature — classical or

quantum-mechanical—of the exciton COM motion subject to the disordered potential.

The first time resolved measurements of RRS under pulsed excitation<sup>7</sup> have shown that the time dependent signal decays with a rate given by the inverse of the exciton homogeneous broadening. However, the time resolution was still too poor to resolve features on the time scale relevant to the scattering process, namely the inverse of the exciton inhomogeneous broadening. Wang *et al.*<sup>8</sup> have resolved the RRS signal on the femtosecond scale. It turned out that the RRS response is not instantaneous and that the maximum in the scattered intensity occurs at a finite time delay. Their measurements, however, were dominated by excitation dependent nonlinear effects which affected the shape of the time resolved signal. Low intensity measurements were performed by Haacke *et al.*<sup>9</sup> In the linear regime the RRS signal presents two remarkable features. First, it rises quadratically in time. In addition, the decay is characterized by a fast non-exponential component on the time scale of the inverse inhomogeneous broadening, followed by a slower exponential decay. In order to explain this behavior, a theoretical model has been adopted which assumes an ensemble of classical oscillators moving within a random potential with finite correlation length. This model accounts for the rise and the fast decay component but underestimates the RRS intensity in the long-time limit. To explain this discrepancy, it was argued that the emitted signal in the nonspecular direction also has a contribution from incoherent photoluminescence originating from relaxation processes. It is not easy, however, to quantitatively estimate the relative importance of the two contributions. As will be pointed out later on, an alternative explanation can be drawn from the quantum-mechanical nature of the localized exciton states. The most recent experimental works on time resolved RRS were aimed at the distinction between the RRS and the incoherent photoluminescence contributions to the radiated field. To this purpose, the coherent properties of the scattered field have

been investigated through interferometric measurements.<sup>10,11</sup> These results, however, have not provided new information about the nature of the exciton localization.

A difficulty inherent in any RRS measurement consists in the fact that all the relevant information on the system must be extracted with the help of an accurate model of the scattering process. Theoretical attempts to describe both steady-state and time dependent RRS signals were based on the assumption of a spatially fluctuating local dielectric function, from which the excitonic polarization was derived.<sup>2,4,7</sup> In addition, Stolz *et al.*<sup>7</sup> have discarded the spectral dependence of the dielectric function, thus obtaining an instantaneous RRS signal. The choice of a local dielectric function corresponds to the assumption of classical motion of the exciton COM, as will be shown in the present treatment. Zimmermann<sup>12</sup> has provided a theoretical account of RRS including quantum-mechanical features of the exciton in-plane motion. The exciton-disorder interaction has been described within a self-consistent second Born approximation. In addition, the disorder has been treated on a most general basis via the introduction of the two-point statistical correlation function of the in-plane potential. It has been shown that, disregarding any homogeneous contribution to the exciton linewidth, the time dependent signal approaches a finite value. In a realistic situation, the decay due to homogeneous processes such as radiative recombination has to be superimposed, which results in a purely exponential decay for long times. The kinetic theory presented in Ref. 12 provides the exact result in the limit of classical exciton motion. An important feature emerging from this treatment is that the shape of the time dependent signal in the quantum-mechanical case coincides with the corresponding classical limit for short times up to the occurrence of the plateau. For later times, the quantum result stays constant while the classical one decays as  $t^{-2}$ . This gives important insight into how quantum-mechanical effects could account for the long-time limit of the experimental results by Haacke *et al.* The formal theory of RRS has also been derived by Citrin<sup>13</sup> who included polaritonic effects in the exciton in-plane motion. The numerical results, however, were again obtained in the classical limit, neglecting the polaritonic effects and with *ad hoc* assumptions for the disordered potential.

The aim of the present paper is to provide a full quantum treatment of RRS due to excitons. The macroscopic polarization originating from the incoming electromagnetic field obeys the Schrödinger equation for the exciton COM motion. The disorder is accounted for by a Gauss distributed random potential assuming an arbitrary two-point correlation function in space. For the numerical results, however, a Gauss correlation function will be assumed. The expression for the scattered field is derived and the angular features are carefully included, separating specular emission from scattering. It is demonstrated that a finite angular acceptance in the detection of the scattered field formally corresponds to averaging the calculated intensity over a statistical ensemble of different potential configurations. The equation for the polarization is solved numerically over a wide range of parameters, from the classical limit to the limit of spatially uncorrelated potential (white noise limit). The results for the RRS intensity are studied both in the frequency and in the time domain. In the frequency domain, the RRS intensity

corresponds to the statistical level-level correlation function for the eigenstates of the COM motion, once the uncorrelated counterpart has been subtracted. This allows us to establish a direct connection between RRS and level repulsion originating from the quantum nature of the COM motion. The corresponding results for the RRS in the time domain give the precise shape of the time resolved field intensity. The main improvement brought about by this exact numerical solution to the second Born results of Ref. 12 consists in the occurrence of a minimum in the time dependent RRS intensity before the plateau is reached. The minimum is shown to be a natural consequence of the quantum-mechanical level repulsion. In reality, this feature could be blurred by the exponential decay of the signal due to homogeneous broadening processes. However, the numerical calculations show that in a regime of low temperature and density, where only the radiative decay contributes, the present result is compatible with the appearance of a double-peaked feature in the time resolved signal. This unique behavior, that has recently been observed,<sup>14</sup> is an unambiguous signature of the quantum-mechanical nature of the exciton COM motion along the disordered QW plane.

The article is organized as follows. In Sec. II we derive the formal theory of Rayleigh scattering by QW excitons. In Sec. III we express the RRS signal in terms of the quantized eigenenergies of the exciton COM motion, while the corresponding classical limit is derived analytically in Sec. IV. Section V is devoted to the presentation and the discussion of the results. In Sec. VI we present the conclusions.

## II. EMITTED FIELD AND TIME RESOLVED INTENSITY

The optics near to the fundamental absorption edge in semiconductor nanostructures is dominated by excitonic effects. We concentrate on the  $1s$  exciton of the lowest heavy-hole subband. The following more general derivations are valid for both quantum wells (QW's) and quantum well wires (QWW's). If needed we distinguish both cases by the spatial dimension  $D=2$  or  $D=1$ , respectively. For the numerical results, however, we restrict ourselves to the one-dimensional (1D) case.

Rayleigh scattering relies on the imperfect spatial structure which might be due to interface roughness and/or alloy disorder. In average quality QW's the amplitude of the confinement energy fluctuations are typically one order of magnitude smaller than the exciton binding energy. In this limit, the relative exciton motion, described by the wave function  $\phi_{1s}(\boldsymbol{\rho})$ , may be assumed as undistorted by disorder.<sup>15</sup> Then, only the COM motion remains to be solved which is accomplished via the Schrödinger equation for the excitonic polarization  $P(\mathbf{R}, t)$ ,

$$-i\hbar\partial_t P(\mathbf{R}, t) = H_{\mathbf{R}} P(\mathbf{R}, t) + \mu E_{in}(\mathbf{R}, t). \quad (1)$$

The COM vector  $\mathbf{R}$  is restricted to lie within the quantum well plane or along the wire direction. Denoting the average  $1s$  exciton energy by  $\hbar\omega_x$ , the Hamilton operator is given by

$$H_{\mathbf{R}} = -\frac{\hbar^2}{2M}\Delta_{\mathbf{R}} + V_{\mathbf{R}} + \hbar\omega_x, \quad (2)$$

with  $M$  being the in-plane kinetic mass of the exciton.  $V_{\mathbf{R}}$  is the random potential felt by the exciton as a whole. It has zero mean value, is Gauss distributed, and correlated over a length approximately given by the exciton Bohr radius as shown elsewhere.<sup>16</sup> We introduce the two-point potential correlation function  $f_{\mathbf{R}}$  via the relation

$$\langle V_{\mathbf{R}} V_{\mathbf{R}'} \rangle = \sigma^2 f_{\mathbf{R}-\mathbf{R}'}, \quad (3)$$

where  $\sigma$  is the width of the Gauss distribution, and  $f_0 = 1$ . The notation  $\langle \dots \rangle$  indicates here and in what follows an average over the statistical ensemble of disorder configurations. We define the potential correlation length  $\xi$  as the length scale over which the correlation function  $f_{\mathbf{R}}$  decays to zero. Hence  $\xi$  constitutes the natural length unit for the Schrödinger problem. A corresponding unit of energy is  $E_c = \hbar^2 \xi^{-2} / 2M$ . In Appendix A we derive the scaling properties of the Schrödinger equation. After rescaling to the above units  $\xi$  and  $E_c$ , there is only one independent parameter in the problem, namely the ratio  $\sigma/E_c$ . At this stage we do not make any further assumption for the disordered potential  $V_{\mathbf{R}}$ . We point out, however, that the (optically active) eigenfunctions of the Hamiltonian Eq. (2) are characterized by a typical localization length,  $l_{loc}$ , that will be used in the following discussion.

The excitonic polarization is driven by the exciting light field  $E_{in}$  via dipole coupling.  $\mu$  contains here — additionally to the interband matrix element—the confinement overlap and the excitonic enhancement  $\phi_{1s}(0)$ .<sup>17</sup> Since the resonant radiation is expected to be angle dependent, the spatial structure of the light field has to be taken into account carefully. The incoming plane wave directed along  $\mathbf{e}_L$  ( $\mathbf{k}_L = \mathbf{e}_L \omega_p / c$ ) is modulated by an amplitude function in time and space,

$$E_{in}(\mathbf{r}, t) = e^{i(\omega_p t - \mathbf{k}_L \mathbf{r})} A(\mathbf{r}, t - \mathbf{e}_L \mathbf{r} / c). \quad (4)$$

A formal integration of the differential equation gives

$$P(\mathbf{R}, t) = \frac{i\mu}{\hbar} \int_0^\infty d\tau e^{iH_{\mathbf{R}} \tau} E_{in}(\mathbf{R}, t - \tau). \quad (5)$$

In what follows we put  $\hbar = 1$ . The polarization is the source of the emitted field at a point  $\mathbf{r}$  outside the sample,<sup>4</sup>

$$E_{out}(\mathbf{r}, t) = -k_L^2 \mu \int d\mathbf{R} \frac{P(\mathbf{R}, t - |\mathbf{r} - \mathbf{R}|/c)}{|\mathbf{r} - \mathbf{R}|}. \quad (6)$$

We have dropped any vector notation of fields. The formulas hold strictly if the scattering direction  $\mathbf{e}_S$ , the incoming one  $\mathbf{e}_L$ , and the sample normal are coplanar, and the field polarization is perpendicular. Using the expansion  $|\mathbf{r} - \mathbf{R}| \approx r - \mathbf{e}_S \mathbf{R}$  for the far-field case and dropping the trivial delay  $r/c$  and some prefactors, the field to be observed in direction  $\mathbf{e}_S$  is

$$\begin{aligned} E_{out}(\mathbf{e}_S, t) &= \int d\mathbf{R} P(\mathbf{R}, t + \mathbf{e}_S \mathbf{R} / c) \\ &= i \int_0^\infty d\tau \int d\mathbf{R} e^{iH_{\mathbf{R}} \tau} E_{in}(\mathbf{R}, t + \mathbf{e}_S \mathbf{R}' / c - \tau) \Big|_{\mathbf{R}' = \mathbf{R}}. \end{aligned} \quad (7)$$

The dummy variable  $\mathbf{R}'$  has been introduced to deal with the operator  $H_{\mathbf{R}}$  properly. Defining the scattered wave vector by  $\mathbf{k}_S = \mathbf{e}_S \omega_p / c$  the explicit result is

$$\begin{aligned} E_{out}(\mathbf{e}_S, t) &= i e^{i\omega_p t} \int_0^\infty d\tau \int d\mathbf{R} e^{i(H_{\mathbf{R}} - \omega_p)\tau} e^{i(\mathbf{k}_S \mathbf{R}' - \mathbf{k}_L \mathbf{R})} \\ &\quad \times A[\mathbf{R}, t - \tau + (\mathbf{k}_S \mathbf{R}' - \mathbf{k}_L \mathbf{R}) / \omega_p] \Big|_{\mathbf{R}' = \mathbf{R}}. \end{aligned} \quad (8)$$

If propagation effects within the sample are negligible [ $(\mathbf{k}_S - \mathbf{k}_L) \mathbf{R} / \omega_p$  small with respect to the pulse length], the field amplitude can be taken as spatially homogeneous over the excitation focus  $\Omega_F$ . The scattered field is thus expressed as an integral over the focus region:

$$\begin{aligned} E_{out}(\mathbf{e}_S, t) &= i e^{i\omega_p t} \int_0^\infty d\tau A(t - \tau) \\ &\quad \times \int_{\Omega_F} d\mathbf{R} e^{i\mathbf{k}_S \mathbf{R}} e^{i(H_{\mathbf{R}} - \omega_p)\tau} e^{-i\mathbf{k}_L \mathbf{R}}. \end{aligned} \quad (9)$$

Although a finite pulse is of importance for the spectral selection of the excitonic region, we consider for simplicity the limit of a deltalike excitation,  $A(t) = A_0 \delta(t)$ , ending up with

$$E_{out}(\mathbf{e}_S, t) = i \Theta(t) A_0 \int_{\Omega_F} d\mathbf{R} e^{i\mathbf{k}_S \mathbf{R}} e^{iH_{\mathbf{R}} t} e^{-i\mathbf{k}_L \mathbf{R}}. \quad (10)$$

We remark that Eq. (10) corresponds to the retarded COM exciton propagator, if we identify  $\Omega_F$  with the finite spatial extent of the system. This result holds when retardation in the electromagnetic field propagation along the QW or QWW is disregarded. The more general result including polaritonic effects, formally derived by Citrin,<sup>13</sup> amounts to replacing Eq. (10) by the retarded exciton propagator including polaritonic self-energy corrections. However, these corrections are unimportant as long as  $\lambda \gg l_{loc}$  holds for the wavelength, and may be safely neglected in the present discussion.

It has been shown recently<sup>18</sup> that the measured time resolved intensity per unit area and per incoming excitation intensity,

$$I(\mathbf{e}_S, t) = \frac{1}{\Omega_F A_0^2} E_{out}^*(\mathbf{e}_S, t) E_{out}(\mathbf{e}_S, t), \quad (11)$$

is randomly fluctuating as a function of detection direction, forming speckles which even depend on time. The angular extension of one speckle is  $\delta_S = 0.44\lambda / L_F$  with  $L_F$  being the full width at half maximum of the Gauss-shaped excitation focus,  $\Omega_F \sim L_F^D$ . The observation angle  $\delta$  is defined relative to the incoming direction,  $\cos \delta = \mathbf{e}_S \cdot \mathbf{e}_L$ .

In any experiment with moderate angular resolution, an average over many speckles is detected, which means to integrate over  $\mathbf{e}_S$  in a small range. By averaging Eq. (11) over a Gauss aperture of  $\delta_A = 0.44\lambda / L_A$ , straightforward algebra leads to

$$\begin{aligned} I(\mathbf{e}_S, t) &= \frac{1}{\Omega_F} \int_{\Omega_F} d\mathbf{R} d\mathbf{R}' e^{-|\mathbf{R} - \mathbf{R}'|^2 \ln 2 / L_A^2} e^{i\mathbf{k}_S(\mathbf{R} - \mathbf{R}')} \\ &\quad \times e^{i(H_{\mathbf{R}} - H_{\mathbf{R}'})t} e^{-i\mathbf{k}_L(\mathbf{R} - \mathbf{R}')}. \end{aligned} \quad (12)$$

The integration is thus effectively restricted to overlapping regions of size  $\Omega_A \sim L_A^D$ .  $L_A$  has to be still larger than the wavelength  $\lambda$  which in turn exceeds  $l_{loc}$  for typical values of the exciton mass and disorder parameters. Therefore the integrations can be carried out independently over units of size  $\Omega_A$ , formally resulting in an average over different disorder realizations,

$$I(\mathbf{e}_S, t) = \frac{1}{\Omega_A} \int_{\Omega_A} d\mathbf{R} d\mathbf{R}' \langle e^{i\mathbf{k}_S(\mathbf{R}-\mathbf{R}')} e^{i(H_{\mathbf{R}}-H_{\mathbf{R}'})t} e^{-i\mathbf{k}_L(\mathbf{R}-\mathbf{R}')} \rangle. \quad (13)$$

This may be viewed upon as a (somewhat unusual) ergodic hypothesis: A directional average can be replaced by an ensemble average. A (residual) smooth angular dependence outside the reflected/transmitted direction would result if  $\lambda$  and  $l_{loc}$  are comparable. However, with the exception of extremely small disorder,  $\lambda \gg l_{loc}$  holds pretty well. As a consequence, the scattered intensity is practically isotropic and it is possible to get rid of the momentum dependence after splitting off the uncorrelated average

$$I_{sc}(t) = \frac{1}{\Omega} \int_{\Omega} d\mathbf{R} d\mathbf{R}' \langle e^{i(H_{\mathbf{R}}-H_{\mathbf{R}'})t} \rangle - \frac{1}{\Omega} \left| \int_{\Omega} d\mathbf{R} \langle e^{iH_{\mathbf{R}}t} \rangle \right|^2, \quad (14)$$

where  $\Omega$  now denotes a still smaller integration domain such that  $\lambda^D \gg \Omega \gg l_{loc}^D$ . The detailed derivation of Eq. (14) is presented in Appendix B.

### III. RAYLEIGH SCATTERING — QUANTIZED

In order to proceed, eigenfunctions of the COM motion  $\psi_{\alpha}(\mathbf{R})$  are introduced,

$$H_{\mathbf{R}} \psi_{\alpha}(\mathbf{R}) = \epsilon_{\alpha} \psi_{\alpha}(\mathbf{R}), \quad (15)$$

which have to be normalized within  $\Omega_A$ . Exploiting the orthonormality, one gets for the intensity Eq. (13)

$$I(\mathbf{e}_S, t) = \frac{1}{\Omega_A} \left\langle \sum_{\alpha, \beta} \psi_{\alpha \mathbf{k}_S}^* \psi_{\alpha \mathbf{k}_L} e^{i(\epsilon_{\alpha} - \epsilon_{\beta})t} \psi_{\beta \mathbf{k}_S} \psi_{\beta \mathbf{k}_L}^* \right\rangle \quad (16)$$

with the Fourier transform of the wave function

$$\psi_{\alpha \mathbf{k}} = \int_{\Omega_A} d\mathbf{R} e^{i\mathbf{k}\mathbf{R}} \psi_{\alpha}(\mathbf{R}) \quad (17)$$

being the COM part of the optical matrix element. As detailed in Appendix B, the scattered intensity equals the correlated part of this expression [cf. Eq. (14)]

$$I_{sc}(t) = \frac{1}{\Omega} \left\langle \sum_{\alpha, \beta} M_{\alpha}^2 M_{\beta}^2 e^{i(\epsilon_{\alpha} - \epsilon_{\beta})t} \right\rangle - \frac{1}{\Omega} \left\langle \sum_{\alpha} M_{\alpha}^2 e^{i\epsilon_{\alpha}t} \right\rangle^2, \quad (18)$$

where  $M_{\alpha} = \int_{\Omega} \psi_{\alpha}(\mathbf{R}) d\mathbf{R}$ . The normalization is now within  $\Omega$ , and using the completeness relation  $\sum_{\alpha} M_{\alpha}^2 = \Omega$  it is easily seen that  $I_{sc}(0) = 0$  holds. It should be pointed out that the optical matrix elements  $M_{\alpha}$  are very small for high-energy eigenstates whose wave functions are rapidly oscillating. Only for eigenvalues close to the band edge (of the order of  $\sigma$ ),  $M_{\alpha}$  reaches sizable values. We introduce the

optical density  $D(E)$  which determines the linear absorption of the inhomogeneously broadened  $1s$  exciton:

$$D(E) = \frac{1}{\Omega} \left\langle \sum_{\alpha} M_{\alpha}^2 \delta(E - \epsilon_{\alpha}) \right\rangle. \quad (19)$$

Indeed, it has been shown<sup>15,19</sup> that the width of the optical density is always below  $\sigma$  (motional narrowing). The upper bound  $\sigma$  is achieved in the classical limit (see below), where  $D(E)$  simply coincides with the statistical distribution of the disordered potential.

At times much larger than  $\sigma^{-1}$ , destructive interference works effectively leaving only the diagonal term  $\alpha = \beta$  in the first sum in Eq. (18) untouched,

$$I_{sc}(t \rightarrow \infty) = \frac{1}{\Omega} \left\langle \sum_{\alpha} M_{\alpha}^4 \right\rangle \equiv L_{opt}^D, \quad (20)$$

which has the dimension of an area or a length in dependence on dimensionality  $D$ . We call  $L_{opt}$  the optically relevant average wave function extension.

For the interpretation of the results as well as for the numerical simulation, it is advantageous to work in the frequency domain. Fourier transforming the time dependence according to

$$I_{sc}(t) = \int dE [R(E) - R_0(E)] \cos(Et) \quad (21)$$

gives from the first part in Eq. (18) a function,

$$R(E) = \frac{1}{\Omega} \left\langle \sum_{\alpha, \beta} M_{\alpha}^2 M_{\beta}^2 \delta[E - (\epsilon_{\alpha} - \epsilon_{\beta})] \right\rangle, \quad (22)$$

which can be considered as the level distance distribution, weighted with the optical matrix elements. The symmetry  $R(E) = R(-E)$  is obvious. Note that the diagonal terms in the double sum of Eq. (22) provide a deltalike contribution,

$$\delta(E) \frac{1}{\Omega} \left\langle \sum_{\alpha} M_{\alpha}^4 \right\rangle = \delta(E) L_{opt}^D, \quad (23)$$

which accounts for the long-time limit of the scattered intensity.

The optical density  $D(E)$  can be used to express the second part of Eq. (18) as a convolution,

$$R_0(E) = \Omega \int dE' D(E') D(E' - E). \quad (24)$$

There is a large compensation between  $R(E)$  and  $R_0(E)$  appearing in Eq. (21). Both contributions scale with the system size  $\Omega$ . However, distant parts of the system are statistically independent from each other and cancel out when forming the difference between correlated and decoupled terms,  $R_c(E) \equiv R(E) - R_0(E)$ . Consequently,  $R_c(E)$  is not an extensive quantity and is well defined in the limit of infinite system size, too. This point will be further elucidated in Sec. V where numerical results for  $R(E)$  and  $R_0(E)$  are presented.

#### IV. RAYLEIGH SCATTERING — CLASSICAL

For a better understanding of the results, it is useful to examine the limit of classical exciton COM motion. Treating excitons as classical particles means to neglect the kinetic term in Eq. (2). More generally, this is justified for large values of  $\sigma/E_c$  which could be reached by heavy excitons, large correlation length of the potential, or strong disorder. Defining the scattering vector  $\mathbf{q}=\mathbf{k}_s-\mathbf{k}_L$ , we have now instead of Eq. (13) simply

$$I(\mathbf{q},t)=\frac{1}{\Omega_A}\int_{\Omega_A}d\mathbf{R}d\mathbf{R}'e^{i\mathbf{q}(\mathbf{R}-\mathbf{R}')}\langle e^{i(V_{\mathbf{R}}-V_{\mathbf{R}'})t}\rangle. \quad (25)$$

The disorder average is performed in Appendix C, it depends solely on the pair-correlation function of the random potential introduced in Eq. (34):

$$I(\mathbf{q},t)=\int_{\Omega_A}d\mathbf{R}e^{i\mathbf{q}\mathbf{R}}\exp[-\sigma^2t^2(1-f_{\mathbf{R}})]. \quad (26)$$

Since  $f_{\mathbf{R}}$  decays to zero rapidly, we subtract and add the limiting behavior and integrate the latter over  $\Omega_A$ ,

$$I(\mathbf{q},t)=e^{-\sigma^2t^2}\int_{\Omega_A}d\mathbf{R}e^{i\mathbf{q}\mathbf{R}}(e^{\sigma^2t^2f_{\mathbf{R}}}-1)+e^{-\sigma^2t^2}\Omega_A\delta_{\mathbf{q},0}. \quad (27)$$

The second part is nonzero only in the specular (reflected or transmitted) direction. In the first part, the spatial integration is essentially restricted to the correlation length  $\xi$ , and due to  $q\xi\ll 1$  the exponential  $e^{i\mathbf{q}\mathbf{R}}$  can be replaced by unity. Outside the specular direction we get the final result,

$$I_{sc}(t)=e^{-\sigma^2t^2}\int_{\Omega}d\mathbf{R}(e^{\sigma^2t^2f_{\mathbf{R}}}-1), \quad (28)$$

where the integration can now be restricted to the simulation size  $\Omega$  as well. The scattered (Rayleigh) signal exhibits therefore no angular dependence if  $\xi\ll\lambda$  holds, which in the classical case replaces the inequality  $l_{loc}\ll\lambda$  used above.

Obviously,  $I_{sc}(t)$  starts quadratically in time, and the time scale is set by  $1/\sigma$ . For large times, the signal decays as  $t^{-D}$  if a Gaussian spatial correlation is assumed. This nontrivial time dependence (rise and decay) stems from the product of time and correlation in the exponent: as time elapses, the range of  $f_{\mathbf{R}}$ , which is probed, diminishes. The classical result for the 2D case has been derived before in Ref. 12.

A simplification assuming time independent spatial correlation of the susceptibility is completely invalid. This explains why Stolz<sup>7</sup> came up in his theory with an instantaneous Rayleigh signal, which decays only via dephasing.

It is instructive that the same final result can be derived starting from the general expression<sup>2</sup>

$$I_{sc}(t)=\langle\chi^*(t)\chi(t)\rangle-\langle\chi^*(t)\rangle\langle\chi(t)\rangle, \quad (29)$$

which states that the scattered intensity is given by the fluctuations of the linear susceptibility. In the present case, an oscillator type is appropriate,

$$\chi(\omega)=\int d\mathbf{R}\frac{1}{V_{\mathbf{R}}+\omega_x-\omega-i0}, \quad (30)$$

or Fourier transformed

$$\chi(t)=i\Theta(t)\int d\mathbf{R}e^{i(V_{\mathbf{R}}+\omega_x)t}. \quad (31)$$

This establishes the connection between the present classical limit and the fluctuating dielectric constant model of Refs. 2, 4, and 7.

We conclude this section with explicit results for the optical level distance distributions, valid for the classical case. Fourier transforming both parts of Eq. (28) gives

$$R^{cl}(E)=\int_{\Omega}d\mathbf{R}\frac{1}{\sqrt{\pi}2\sigma\sqrt{1-f_{\mathbf{R}}}}e^{-E^2/[4\sigma^2(1-f_{\mathbf{R}})]} \quad (32)$$

and

$$R_0^{cl}(E)=\frac{\Omega}{\sqrt{\pi}2\sigma}e^{-E^2/4\sigma^2} \quad (33)$$

as the decoupled part. Both expressions scale with the system size  $\Omega$ , but their difference does not. This can be seen using the limit  $f_{\mathbf{R}}\rightarrow 0$  for large argument, and corroborates the general statement made at the end of the preceding section.

#### V. RESULTS

All calculations presented here refer to the one-dimensional case ( $D=1$ ), which refers to the continuous Anderson model with correlated disorder. We do not go into the details of how the relative exciton wave function in the quantum wire is averaging over the underlying atomic-scale disorder.<sup>16</sup> Rather, we assume a potential correlation of Gauss type,

$$f_{\mathbf{R}}=\exp(-R^2/2\xi^2). \quad (34)$$

To give physical units, we adopt an exciton kinetic mass of  $M=0.25 m_0$  typical for AlAs/GaAs quantum wells. With a potential correlation length of  $\xi=10$  nm, for example, the reference energy is  $E_c=1.5$  meV. Large-scale numerical simulations have been performed for determining eigenfunctions and eigenvalues. The second derivative in Eq. (2) has been discretized on a fine grid, mapping the problem to an effective tight-binding calculation. Step size  $\Delta$  as well as chain length have been carefully adjusted in order to avoid finite-size effects. In particular, two prescriptions have been adopted for dealing properly with a continuous potential. First, the system size  $\Omega=L$  was always chosen much larger than  $l_{loc}$  (we found  $L=4 \mu\text{m}$  sufficient in all cases). Second, the transfer energy  $T=\hbar^2\Delta^{-2}/2M$  was taken much larger than both  $\sigma$  and  $E_c$ . The latter prescription assures that both the kinetic and the potential terms in the Schrödinger equation are sampled sufficiently dense.

The first quantity we study is the optical length  $L_{opt}$  which we calculate for varying values of  $\sigma$  and  $E_c$ . Because of the scaling properties of the Schrödinger equation (Appendix A), any length of the system scales as  $\xi F(\sigma/E_c)$ , where  $F$  denotes a specific dimensionless function. We thus plot in Fig. 1 the optical length  $L_{opt}/\xi$  as a function of  $\sigma/E_c$  on a double logarithmic scale. For this calculation, the sys-

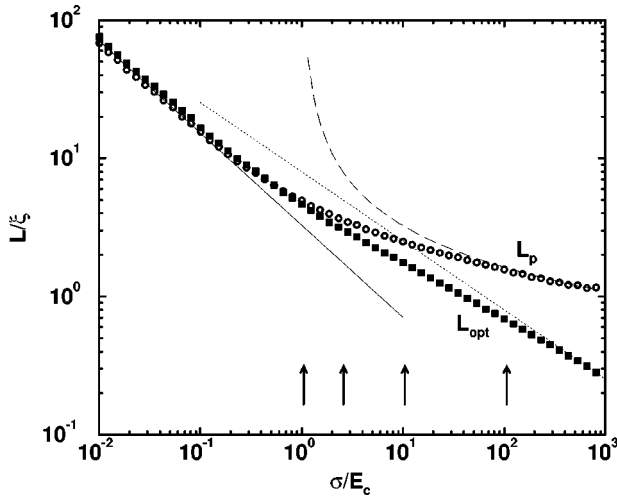


FIG. 1. Optical length  $L_{opt}$  (squares) and inverse participation length  $L_p$  (open circles) as a function of  $\sigma/E_c$ . The points have been calculated varying both  $\sigma$  and  $E_c$ , but follow two well defined curves, as expected from the scaling properties. The asymptotic behavior is depicted by thin curves (see text). The arrows indicate the parameter values used in Fig. 3 and Fig. 4.

tem size  $L$  has been divided into 2048 steps ( $T=40$  meV). Then, both  $\sigma$  and  $\xi$  have been varied within the bounds imposed by the above-mentioned prescriptions. Each point in the plot represents an average over 50 statistically independent potential realizations, and the convergence has been thoroughly checked.

Two limiting cases are of importance. At  $\sigma/E_c \rightarrow \infty$ , we approach the classical limit, where analytical results are available. In the other extreme,  $\sigma/E_c \rightarrow 0$ , the wave functions extend very far ( $l_{loc} \gg \xi$ ), and the white-noise limit is reached (see Appendix A). As shown there, any length has to be a constant time  $\xi(E_c/\sigma)^{2/3}$ . The calculated optical length in Fig. 1 shows clearly the approach to this power-law dependence (full line) for  $\sigma \ll E_c$ .

Among different possibilities, wave function localization can be characterized by the inverse participation ratio.<sup>20</sup> Averaging over the optically active states in a similar fashion<sup>21</sup> as in Eq. (20), we define

$$1/L_p = \frac{1}{\Omega} \left\langle \sum_{\alpha} M_{\alpha}^2 \int d\mathbf{R} \psi_{\alpha}^4(\mathbf{R}) \right\rangle, \quad (35)$$

which gives a result surprisingly close to  $L_{opt}$  in the white-noise limit.

We have searched for asymptotic results close to the classical limit, too ( $\sigma \gg E_c$ ). The eigenfunction in this case piles up in the vicinity of the classical turning points. Concentrating on that part we looked for the linear potential  $V(x) - \epsilon = \sigma x/\xi$  with coefficients solely dictated by dimensional arguments. From the properties of the Airy function solution  $\text{Ai}(\xi(E_c/\sigma)^{1/3})$  we derived as limiting behavior

$$L_{opt} \sim \xi \sqrt{E_c/\sigma} \quad \text{and} \quad L_p \sim \xi/\ln(E_c/\sigma). \quad (36)$$

These findings are backed again by the numerics, as shown in Fig. 1 by a dotted and a dashed curve, respectively.

In view of the present results, we consider the optical length  $L_{opt}$  as a well defined and useful quantity, which

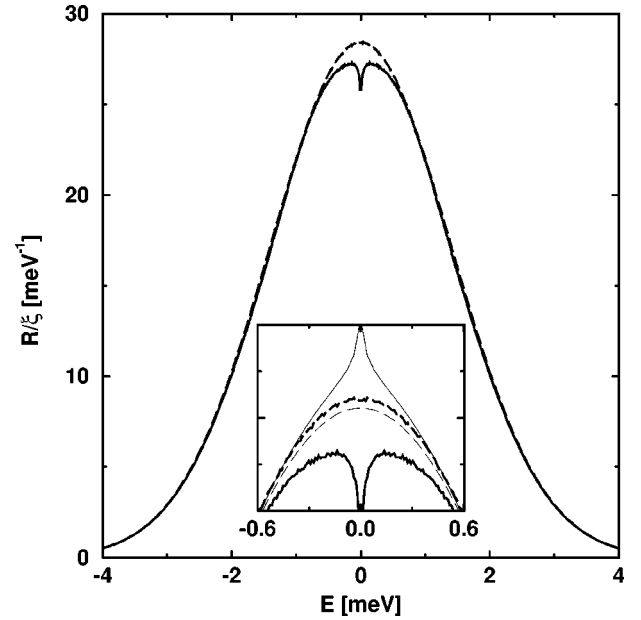


FIG. 2. The optical level distance distribution  $R(E)$  (full curve) and its decoupled counterpart  $R_0(E)$  (dashed curve) in dependence on energy, for  $\sigma/E_c=10$ . The inset shows the important region of small level distances  $E$ , here together with the classical results Eqs. (32) and (33) plotted as thin lines ( $\xi=40$  nm,  $L=4$   $\mu$ m).

serves to characterize the localization of the wave functions in its relevance for optical transitions.

Results for the optical level distance distribution are given in Fig. 2. In this plot, the curves corresponding to the classical limit have been calculated analytically, according to the expressions given in Sec. IV. The numerical calculations for the general case, in this and in the following figures, have been performed by using a system size of  $L=4$   $\mu$ m divided into 512 steps, and  $\sigma=1$  meV. The parameter  $\sigma/E_c$  has been adjusted by varying the correlation length  $\xi$ . Each plot results from an average over  $10^5$  statistically independent realizations. Still, there is some noise left which — in physical terms — can be considered as a remainder of speckle effects. For classical excitons,  $R(E)$  is a smooth curve diverging logarithmically at  $E=0$  due to the spatial correlation in the random potential [Eq. (32)]. This peak is missing in its uncorrelated counterpart  $R_0(E)$ . In the full quantum treatment, however,  $R(E)$  goes sharply down at  $E \rightarrow 0$ , reflecting the “avoided level crossing” behavior of quantum systems. Note that the present expression is weighted by the optical matrix elements, thus emphasizing the optically active COM states close to the band edge. This contrasts the standard definition of unbiased level repulsion elaborated, e.g., in random matrix theory.<sup>22</sup> Recently it has been suggested that the level repulsion feature could be directly detected in microphotoluminescence measurement under steady-state excitation.<sup>23</sup> Here we show how direct evidence of level repulsion is also present in the time resolved intensity.

Figure 3 shows the quantity  $R_c(E)$  for different values of  $\sigma/E_c$ , together with the classical limit plotted as a thin line. The transition from a full quantum situation, close to the white-noise limit, to the classical limit clearly appears. In particular, for values of  $\sigma/E_c \leq 1$ , the curve is always negative, reflecting strong energy-level repulsion. The classical

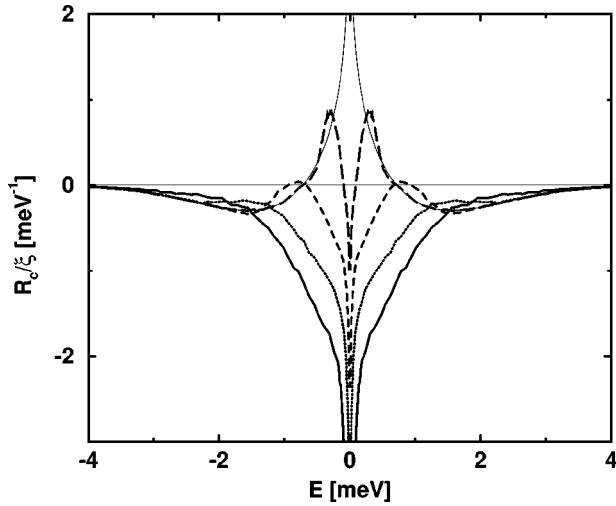


FIG. 3. The subtracted optical level distance distribution  $R_c(E) = R(E) - R_0(E)$  in dependence on energy is plotted for parameter values of  $\sigma/E_c = 1, 2.6, 10, 100$  from below as thick curves. At  $\sigma/E_c = 100$ , the approach to the corresponding classical limit (thin curve) is obvious, but the level repulsion dip close to  $E = 0$  always persists.

limit is approached at large  $|E|$  and the energy interval where the result differs from such limit becomes smaller as  $\sigma/E_c$  increases. As a consequence, a peaked structure develops in an intermediate energy range, while for  $E \rightarrow 0$  a downward level repulsion feature (singularity) is always present, reflecting the quantum nature of the system. The total integral over  $R_c(E)$  including the delta contribution at  $E = 0$  adds up to zero, which accounts for  $I_{sc}(t = 0) = 0$ . The same integral without including the delta contribution is then equal to  $-L_{opt}$ . Thus the value of the optical length  $L_{opt} \equiv I_{sc}(t \rightarrow \infty)$  gives already a rough approximation of the integral level repulsion effect. For the classical curve, we remark that the positive peak at  $E = 0$  is simply related to the spatial correlation of the potential. Similarly, the negative features at larger  $|E|$  only appear in order to preserve level counting (vanishing integral of the curve).

From the experimental point of view, however, this quantity is not accessible through the measurement of the time resolved RRS intensity. In fact, an intrinsic damping of the signal due to radiative as well as nonradiative processes is always present and the measured signal vanishes exponentially.<sup>9</sup> Indeed, it might be objected that a nonzero scattered intensity  $I_{sc}(t \rightarrow \infty)$  for a finite exciting pulse violates energy conservation. However, the overall Rayleigh signal is proportional to the interband optical matrix element, which also determines the radiative exciton recombination rate. Thus in a realistic physical situation RRS is always associated to a finite exciton damping rate that has been disregarded, for clarity, in the present treatment.

Experimental evidence of the quantum level repulsion could be extracted anyway from the time resolved signal. In fact, if converted into the time domain by the Fourier transform, Eq. (21), a nonmonotonic time dependence for the scattered intensity evolves (Fig. 4). The classical result peaks at  $\sigma t = 1.4$  before tending to zero as  $1/t$ . At decreasing values of  $\sigma/E_c$ , the signal follows the classical curve surprisingly far before turning to the nonzero end value, and a minimum

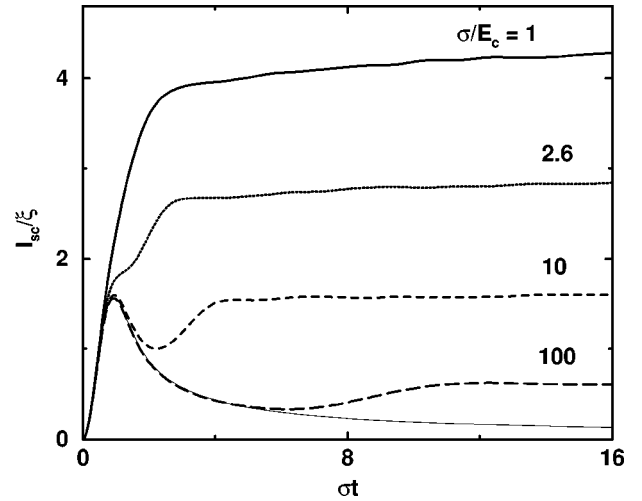


FIG. 4. The scattered Rayleigh intensity  $I_{sc}(t)$  as a function of time is plotted for the same parameters as in Fig. 3, together with the classical limit (thin curve).

appears. A faint oscillation is seen, too, the period of which is related to the peak distance from zero energy in Fig. 3. Consequently, minimum and oscillation are a fingerprint of the level repulsion effect.<sup>24</sup> At still smaller values of  $\sigma/E_c$ , no minimum is seen, but the curve approaches the long-time limit rather slowly. Again, this slow increase is closely related to the small width of the level repulsion dip in energy space.

This analysis provides a key for the interpretation of the experimental results by Haacke *et al.*<sup>9</sup> In that experiment, the measured time dependent intensity was in excess with respect to the prediction of the classical RRS model. The excess intensity was attributed to incoherent photoluminescence originating from inelastic scattering processes. Although the incoherent photoluminescence contribution is always present, this distinction is in general unjustified, as the present results suggest. Indeed, the classical model provides a lower limit to the intensity of the RRS contribution to secondary emission, as Fig. 4 shows. In general, given the typical values of  $M$ ,  $\sigma$ , and  $\xi$  in realistic QW's, we expect the parameter  $\sigma/E_c$  to lie well below 100, thus providing a sizeable increase of the signal at  $\sigma t > 1$  with respect to the classical limit. These considerations should rule out the possibility of distinguishing between coherent and incoherent contribution to secondary emission simply via a subtraction procedure, due to the difficulty in making accurate quantitative predictions of the RRS time dependent signal. Instead, recent studies have shown that this distinction can be made using interferometric techniques<sup>11</sup> or by means of a statistical analysis of the angular intensity fluctuations (speckles).<sup>18</sup> These experiments usually have access to extremely small angular detection windows, thus detecting light from a single speckle of angular extension  $\delta_s$ , in contrast with the angular average assumed here. In particular, in Ref. 11 it was argued that the configuration averaging is based on an *ad hoc* ergodic assumption which could not account for the phase coherence of the RRS. The present model, however, includes only a fully phase-coherent process, namely, light scattering by disordered exciton wave functions. We have rigorously proven that configuration average is not an *ad hoc* assump-

tion and is justified in terms of the angular resolution of typical measurement schemes detecting many speckles at a time. In experiments such as the one by Birkedal *et al.*,<sup>11</sup> the conditions for angular averaging simply do not hold and no relation can be established with the present results. However the present formalism, if applied without carrying out the configuration average, would be appropriate to the description of single speckle RRS measurements.

## VI. CONCLUSIONS

Time resolved resonant Rayleigh scattering of excitons in a disorder-dominated sample offers a unique possibility for detecting level repulsion features. In practice, as already mentioned, radiative recombination together with inelastic-scattering effects will lead to a more or less exponential decay of the scattered intensity, thus making an extraction of fine features a difficult task. However, we have shown in the present work that level repulsion is responsible for a qualitative change in the scattered signal with respect to the classical and white-noise limits. In particular, the inclusion of radiative damping in the form of an exponentially decaying factor, would result in a doubly peaked feature if applied, for example, to the  $\sigma/E_c=10$  curve of Fig. 4. This feature should be easily detected in time resolved RRS measurements with femtosecond resolution, especially in samples fabricated using the growth interruption technique. In fact, it has been suggested<sup>25,26</sup> that this technique should produce interface roughness with rather large correlation length. Indeed, recent Rayleigh scattering measurements on a 9.5-nm-wide quantum well sample with small inhomogeneous width ( $\sigma=0.6$  meV) revealed rather clearly a double peaked feature in the scattered intensity which could be successfully attributed to the level repulsion.<sup>14</sup>

The present results should thus encourage new measurements of time resolved RRS on samples coming from different growth facilities. In fact, in the light of our theory, these measurements might provide better understanding of the properties of heterointerfaces and of the epitaxial growth process.

## ACKNOWLEDGMENTS

We are grateful to C. Ciuti, S. Haacke, C. Piermarocchi, A. Quattropani, E. Runge, and P. Schwendimann for fruitful discussions. V.S. acknowledges support from the Swiss Priority Project ‘‘Optics.’’

## APPENDIX A: SCALING PROPERTIES

The exciton COM problem defined by the Hamiltonian Eq. (2) and the potential correlation Eq. (3) depends on the three parameters  $M$ ,  $\xi$ , and  $\sigma$ , once the type of the correlation function is given. However, the scaling properties of the Schrödinger equation leave only one relevant parameter in the problem. Let us introduce the dimensionless coordinate  $\mathbf{X}=\mathbf{R}/\xi$  which transforms the Laplace operator according to  $\Delta_{\mathbf{R}}=(1/\xi^2)\Delta_{\mathbf{X}}$ . Dividing the Schrödinger equation by

$$E_c = \frac{\hbar^2}{2M\xi^2} \quad (\text{A1})$$

we get

$$(-\Delta_{\mathbf{X}} + \tilde{V}_{\mathbf{X}} - \tilde{\epsilon})\tilde{\psi}(\mathbf{X}) = 0. \quad (\text{A2})$$

The tilde denotes scaled quantities with  $\xi$  as length unit and  $E_c$  as energy unit. The potential correlation is now given by

$$\langle \tilde{V}_{\mathbf{X}} \tilde{V}_{\mathbf{X}'} \rangle = (\sigma/E_c)^2 \tilde{f}_{\mathbf{X}-\mathbf{X}'}, \quad (\text{A3})$$

with the scaled correlation function  $\tilde{f}_{\mathbf{X}}=f_{\mathbf{R}=\xi\mathbf{X}}$ . It is then clear that the (rescaled) problem is uniquely determined by the single dimensionless ratio  $\sigma/E_c$ .

In the white-noise limit, the potential is delta correlated,

$$\langle V_{\mathbf{R}} V_{\mathbf{R}'} \rangle = w \delta(\mathbf{R} - \mathbf{R}'), \quad (\text{A4})$$

where  $w$  has dimensions  $E^2 \cdot L^D$ . Now, the number of independent parameters has been reduced to two,  $w$  and  $M$ . In one dimension we can thus define length and energy units as

$$l_0 = \left( \frac{\hbar^2/2M}{w^{1/2}} \right)^{2/3}, \quad E_0 = \left( \frac{w^2}{\hbar^2/2M} \right)^{1/3}. \quad (\text{A5})$$

The white-noise limit is obtained from the general case in the limit  $\sigma/E_c \ll 1$  which can be reached by very light mass, very short correlation length, or very weak disorder. A precise relation between  $w$ ,  $\sigma$ , and  $\xi$  is established by performing the limit  $\xi \rightarrow 0$  carefully. In the case of a Gauss correlated potential, we have  $f_R = \exp(-R^2/2\xi^2) \rightarrow \sqrt{2\pi}\xi \delta(R)$ . Thus  $w = \sqrt{2\pi}\xi\sigma^2$  holds for a Gauss correlated problem in  $D=1$ . Replacing into Eq. (A5) gives

$$l_0 = \xi(2\pi)^{-1/6} \left( \frac{\sigma}{E_c} \right)^{-2/3}, \quad E_0 = \sigma \left( 2\pi \frac{\sigma}{E_c} \right)^{1/3}. \quad (\text{A6})$$

Approaching the white-noise limit, all the quantities having dimension of a length or an energy must be proportional to  $l_0$  and  $E_0$ , respectively. This limit is correctly reproduced for the optical length  $L_{opt}$  and the optically averaged inverse participation ratio  $L_p$ , as shown in Fig. 1.

## APPENDIX B: LONG-WAVE LIMIT

To simplify the derivation we assume normal incidence,  $\mathbf{k}_L \mathbf{R} = 0$ . The spatial integrations in

$$I(\mathbf{e}_S, t) = \frac{1}{\Omega_A} \int_{\Omega_A} d\mathbf{R} d\mathbf{R}' \langle e^{i\mathbf{k}_S(\mathbf{R}-\mathbf{R}')} e^{i(H_{\mathbf{R}}-H_{\mathbf{R}'})t} \rangle \quad (\text{B1})$$

are split into small units of size  $\Omega = \Omega_A/N$  centered at  $\mathbf{R}_j$ ,

$$I(\mathbf{e}_S, t) = \frac{1}{N\Omega} \sum_{j,l=1}^N e^{i\mathbf{k}_S(\mathbf{R}_j-\mathbf{R}'_l)} \times \int_{\Omega} d\mathbf{R} d\mathbf{R}' \langle \exp i(H_{\mathbf{R}+\mathbf{R}_j} - H_{\mathbf{R}'+\mathbf{R}'_l})t \rangle. \quad (\text{B2})$$

Since  $\Omega$  is taken small compared to the wavelength scale, the phase factors  $\exp(i\mathbf{k}_S \mathbf{R})$  could be omitted. On the other hand,  $\Omega$  is assumed to be large with respect to the relevant localization lengths. Then, only a minor fraction of states spills over into neighboring units, and the average factorizes for the nondiagonal terms  $j \neq l$ . Singling out the diagonal terms  $j=l$  gives

$$I(\mathbf{e}_S, t) = \frac{1}{\Omega} \int_{\Omega} d\mathbf{R} d\mathbf{R}' \langle \exp i(H_{\mathbf{R}} - H_{\mathbf{R}'} t) \rangle + \frac{1}{N\Omega} \sum_{j \neq l} e^{i\mathbf{k}_S(\mathbf{R}_j - \mathbf{R}_l)} \int_{\Omega} d\mathbf{R} \langle e^{iH_{\mathbf{R}} t} \rangle \int_{\Omega} d\mathbf{R}' \langle e^{-iH_{\mathbf{R}'} t} \rangle. \quad (\text{B3})$$

Simplifications were possible since the ensemble average does not depend on the center position. The second line nearly contains the Kronecker delta,

$$\sum_{j,l=1}^N \exp i(\mathbf{k}_S - \mathbf{k}_L)(\mathbf{R}_j - \mathbf{R}_l) = N^2 \delta_{\mathbf{k}_S, \mathbf{k}_L}. \quad (\text{B4})$$

Subtracting and adding the missing term  $j=l$  gives

$$I(\mathbf{e}_S, t) = \frac{1}{\Omega} \left( \int_{\Omega} d\mathbf{R} d\mathbf{R}' \langle e^{i(H_{\mathbf{R}} - H_{\mathbf{R}'} t)} \rangle - \left| \int_{\Omega} d\mathbf{R} \langle e^{iH_{\mathbf{R}} t} \rangle \right|^2 \right) + N\Omega \delta_{\mathbf{k}_S, \mathbf{k}_L} \left| \frac{1}{\Omega} \int_{\Omega} d\mathbf{R} \langle e^{iH_{\mathbf{R}} t} \rangle \right|^2. \quad (\text{B5})$$

The last term represents the specular contribution of the emitted radiation, with the proper scaling of the total area

$\Omega_A = N\Omega$ . Outside  $\mathbf{k}_S = \mathbf{k}_L$ , the scattered intensity has no angular dependence, and Eq. (14) evolves. The condition to be satisfied was  $\lambda^D \gg \Omega \gg l_{loc}^D$  which can be realized since  $\lambda \gg l_{loc}$  holds.

### APPENDIX C: STATISTICS OF POTENTIAL CORRELATION

To perform averages of correlated Gaussian random variables  $V_{\mathbf{r}}$  with zero mean, a useful expression is

$$\left\langle \exp \left( \int d\mathbf{r} h(\mathbf{r}) V_{\mathbf{r}} \right) \right\rangle = \exp \left( \frac{1}{2} \int d\mathbf{r} d\mathbf{r}' h(\mathbf{r}) g_{\mathbf{r}-\mathbf{r}'} h(\mathbf{r}') \right) \quad (\text{C1})$$

which holds for any function  $h(\mathbf{r})$ . The potential correlation function is here defined as  $g_{\mathbf{r}-\mathbf{r}'} = \langle V_{\mathbf{r}} V_{\mathbf{r}'} \rangle$ . Putting

$$h(\mathbf{r}) = it \delta(\mathbf{r} - \mathbf{R}) - it \delta(\mathbf{r} - \mathbf{R}') \quad (\text{C2})$$

gives for the statistical average needed in Eq. (25)

$$\langle \exp(-iV_{\mathbf{R}} t + iV_{\mathbf{R}'} t) \rangle = \exp(-t^2 g_0 + t^2 g_{\mathbf{R}-\mathbf{R}'}). \quad (\text{C3})$$

- 
- <sup>1</sup>R. Loudon, *The Quantum Theory of Light* (Oxford Science Publications, Oxford, 1983).
- <sup>2</sup>J. Hegarty, M. D. Sturge, C. Weisbuch, A. C. Gossard, and W. Wiegmann, *Phys. Rev. Lett.* **49**, 930 (1982).
- <sup>3</sup>J. Hegarty, L. Goldner, and M. D. Sturge, *Phys. Rev. B* **30**, 7346 (1984).
- <sup>4</sup>H. Stolz, *Time-Resolved Light Scattering from Excitons*, Springer Tracts in Modern Physics, Vol. 130, edited by R. D. Pecci, F. Steiner, J. Trümper, and P. Wölfe (Springer, Berlin, 1994).
- <sup>5</sup>M. Gurioli, F. Bogani, A. Vinattieri, M. Colocci, V. I. Belitsky, A. Cantarero, and S. T. Pavlov, *Solid State Commun.* **97**, 389 (1996).
- <sup>6</sup>N. Garro, L. Pugh, R. T. Phillips, V. Drouot, M. Y. Simmons, B. Kardynal, and D.A. Ritchie, *Phys. Rev. B* **55**, 13 752 (1997).
- <sup>7</sup>H. Stolz, D. Schwarze, W. von der Osten, and G. Weimann, *Phys. Rev. B* **47**, 9669 (1993).
- <sup>8</sup>H. Wang, J. Shah, T. Damen, and L. Pfeiffer, *Phys. Rev. Lett.* **74**, 3065 (1995).
- <sup>9</sup>S. Haacke, R. A. Taylor, R. Zimmermann, I. Bar-Joseph, and B. Deveaud, *Phys. Rev. Lett.* **78**, 2228 (1997).
- <sup>10</sup>M. Gurioli, F. Bogani, S. Ceccherini, and M. Colocci, *Phys. Rev. Lett.* **78**, 3205 (1997).
- <sup>11</sup>D. Birkedal and J. Shah, *Phys. Rev. Lett.* **81**, 2372 (1998).
- <sup>12</sup>R. Zimmermann, *Nuovo Cimento D* **17**, 1801 (1995).
- <sup>13</sup>D. S. Citrin, *Phys. Rev. B* **54**, 14 572 (1996).
- <sup>14</sup>V. Savona, St. Haacke, and B. Deveaud (unpublished).
- <sup>15</sup>R. Zimmermann, *Phys. Status Solidi B* **173**, 129 (1992).
- <sup>16</sup>R. Zimmermann, F. Grosse, and E. Runge, *Pure Appl. Chem.* **69**, 1179 (1997).
- <sup>17</sup>F. Tassone, F. Bassani, and L. C. Andreani, *Nuovo Cimento D* **12**, 1673 (1990).
- <sup>18</sup>W. Langbein, J. M. Hvam, and R. Zimmermann, *Phys. Rev. Lett.* **82**, 1040 (1999).
- <sup>19</sup>S. Glutsch and F. Bechstedt, *Phys. Rev. B* **50**, 7733 (1994).
- <sup>20</sup>D. J. Thouless, *Phys. Rep., Phys. Lett.* **C13**, 93 (1974).
- <sup>21</sup>The alternative of weighing  $1/\int d\mathbf{R} \psi_{\alpha}^4(\mathbf{R})$  with  $M_{\alpha}^2$  gave much larger lengths compared to  $L_{opt}$ , and has been discarded.
- <sup>22</sup>M. L. Mehta, *Random Matrices*, 2nd ed. (Academic Press, San Diego, 1990).
- <sup>23</sup>E. Runge and R. Zimmermann, *Adv. Solid State Phys.* **38**, 251 (1998).
- <sup>24</sup>In Ref. 12, no minimum in the scattered intensity has been found. We conclude that the kinetic approach used there, while reproducing the classical limit exactly, fails to include the level repulsion effect for  $E_c > 0$ .
- <sup>25</sup>U. Jahn, S. H. Kwok, M. Ramsteiner, R. Hey, H. T. Grahn, and E. Runge, *Phys. Rev. B* **54**, 2733 (1996).
- <sup>26</sup>D. Gammon, E. S. Snow, B. V. Shanabrook, D. S. Katzer, and D. Park, *Phys. Rev. Lett.* **76**, 3005 (1996).